

Cite this: DOI: 10.1039/c0xx00000x

www.rsc.org/xxxxxx

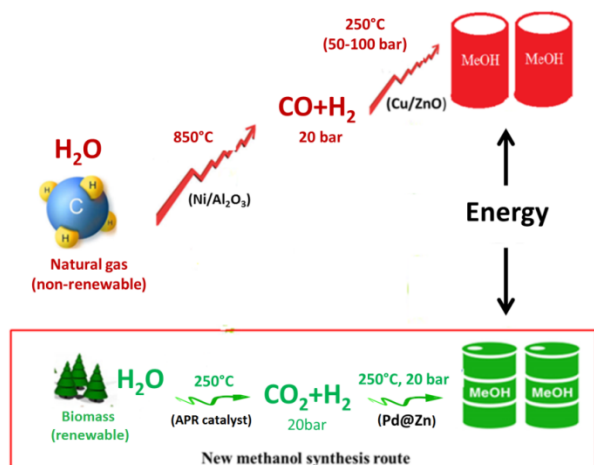
## ARTICLE TYPE

# A Low Pressure Methanol Synthesis Based on Biomass Reforming over Pd@Zn Core-Shell Catalysts

Fenglin Liao,<sup>a</sup> Xin-Ping Wu,<sup>b</sup> Jianwei Zheng,<sup>c</sup> Molly Meng-Jung Li,<sup>a</sup> Andrew Dent,<sup>d</sup> Ziyang Zeng,<sup>e</sup> Xinlin Hong,<sup>e</sup> Anna Kroner,<sup>d</sup> Youzhu Yuan,<sup>c</sup> Xue-Qing Gong,<sup>b\*</sup> Shik Chi Edman Tsang<sup>a\*</sup>

Received (in XXX, XXX) Xth XXXXXXXXXX 20XX, Accepted Xth XXXXXXXXXX 20XX  
DOI: 10.1039/b000000x

At present, there is no low pressure methanol process from CO<sub>2</sub>/H<sub>2</sub> despite the fact that an upstream process of aqueous phase reforming (APR) of biomass derivatives at industrial scale for CO<sub>2</sub>/H<sub>2</sub> production at ~2 MPa is demonstrated. This is due to unfavorable thermodynamics and particularly high CO levels produced through reversed water gas shift reaction for most studied catalysts. Here we report that a new Pd@Zn core-shell catalyst which offers a significantly higher kinetic barrier for CO/H<sub>2</sub>O formation in CO<sub>2</sub> hydrogenation to reduce CO levels but facilitates CH<sub>3</sub>OH formation at or below 2 MPa with CH<sub>3</sub>OH selectivity maintained at ca. 70% as compared to 10% over industrial Cu catalysts. The turnover frequency per Pd over Pd@Zn is 1.9×10<sup>-1</sup> s<sup>-1</sup>, which is about 350 times higher than that of Cu counterpart. It is thus believed this active Pd based catalyst opens up a promising possibility for low pressure and low temperature methanol production using renewable biomass resource for fossil-fuels-starved countries, as shown in Scheme 1.



**Scheme 1.** A renewable-based low temperature, low pressure methanol production process *via* catalytic hydrogenation of CO<sub>2</sub> over Pd@Zn in comparison with traditional syngas route over Cu/ZnO.

Catalytic methanol production is one of the most important reactions in industry due to the wide applications of methanol in chemicals synthesis.<sup>1,2</sup> Currently, methanol is produced by two

steps, namely a high temperature process is required to break down the resilient methane molecule (natural gas) to synthesis gas (CO/H<sub>2</sub> syngas) by steam reforming over Ni based catalyst at >850 °C, 2 MPa and then the syngas is rearranged to methanol over Cu/ZnO catalyst at 250 °C, 5-10 MPa.<sup>3,4</sup> Thus, this process is non-renewable, energy inefficient and the conditions for the two steps are non-compatible with each other.<sup>5-7</sup> Particularly, the latter step of transforming synthesis gas into methanol requires a higher pressure, and thus, the cost for pumping and cumbersome equipment significantly reduces the profit margins.

Owing to the exhaustion of fossil fuels and the accompanying emission of CO<sub>2</sub> as the primary greenhouse gas,<sup>8,9</sup> it would be attractive to use renewable methanol as a chemical platform for future fuels and chemicals production. The process is so called ‘methanol economy’ which is carbon neutral.<sup>1</sup> As one of the primary renewable energy resources, biomass is regarded as a promising alternative for the fossil fuels.<sup>10</sup> The low temperature aqueous phase reforming (APR) of biomass derivatives at industrial scale for CO<sub>2</sub>/H<sub>2</sub> production at 2 MPa is recently demonstrated.<sup>11</sup> Thus, the downstream catalytic CO<sub>2</sub> hydrogenation to methanol (CO<sub>2</sub> + 3H<sub>2</sub> → CH<sub>3</sub>OH + H<sub>2</sub>O) under similar conditions to couple with the above CO<sub>2</sub>/H<sub>2</sub> processes would be highly desirable. Much of the current research is being focused on Cu catalysts for this reaction. As reviewed by Saito,<sup>12</sup> Cu/ZnO based catalysts not only appear to be active for CO/H<sub>2</sub> conversion but they also exhibit superior activity in CO<sub>2</sub> hydrogenation to methanol among a wide variety of catalysts. Unfortunately, CO can be favorably produced through the reversed water gas shift reaction (RWGS) route (CO<sub>2</sub> + H<sub>2</sub> → CO + H<sub>2</sub>O) during methanol synthesis, especially under low pressure conditions. For Cu-based catalysts, methanol selectivity above 50% commonly requires a pressure over 5-10 MPa.<sup>12</sup> When a pressure is set at or below 2 MPa, the rate of RWGS is generally 1-3 order of magnitude higher than that of methanol formation over CuZn,<sup>13</sup> leading to an extremely low methanol selectivity. We are therefore interested in exploring non-Cu based catalysts for methanol synthesis at mild conditions. For the alternative catalysts, Pd commonly shows similar catalytic properties as Cu upon modification but is less susceptible to sintering and poisoning. However, typical reduced Pd/ZnO catalysts were not selective for methanol synthesis (see results later) neither due to the co-existence of RWGS. In this communication, we report that a series of Pd@Zn core-shell nano-structures with variable

composition shows a progressively enhanced ability in suppressing the RWGS selectively with increasing Zn content. The samples were prepared via a CdSe method: CdSe quantum dot was added into the Pd/ZnO system to modify the reduction behaviour of ZnO support in the H<sub>2</sub> pre-treatment and consequently various amount of Zn atoms were derived from the refractory support to decorate on the surface of Pd particles. The existence of CdSe in ZnO support was confirmed by the X-ray diffraction pattern, and is shown in Figure S1.

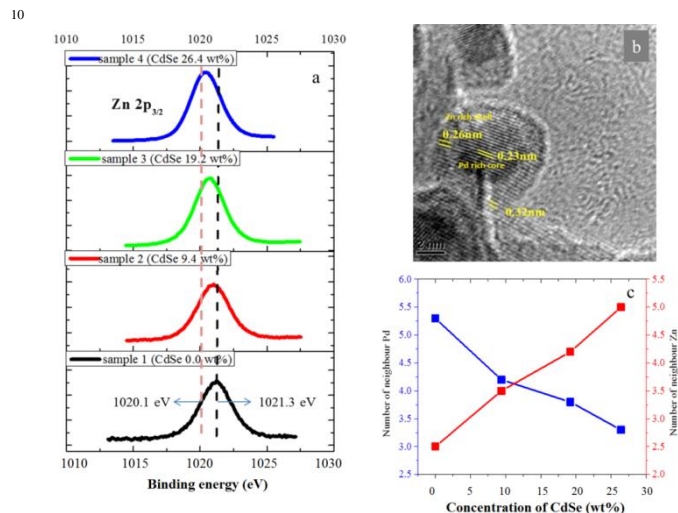


**Fig.1 a.** XPS curves of Zn in a series of reduced Pd/ZnO-CdSe (5 wt% Pd) samples (dotted line indicates the binding energy of Zn<sup>2+</sup> (1021.3 eV) and Zn(0) (1020.1 eV) with reference to the added boron nitride (BN), N 398.2 eV); the corresponding XPS curves of Pd are shown in Figure S2; **b.** A typical HRTEM image of reduced sample 4 (5 wt% Pd, 26.4 wt% CdSe). **1c.** The number of neighbouring Pd (NPd) and Zn (NZn) around each Pd absorbing atom derived from the EXAFS.

The Zn X-ray photoelectron spectra (XPS) of a series of reduced Pd/ZnO-CdSe samples shown in Fig. 1a clearly indicates a downshift of binding energy. This implies that the surface concentration of Zn(0) increases at the expense of Zn(2+) upon reduction with increasing CdSe content doped in Pd/ZnO. The transmission electron microscopy (TEM) images of reduced sample 4 (5 wt% Pd, 26.4 wt% CdSe) with the highest concentration of CdSe depict an imperfect core (dark)-shell (light) structure (Fig. 1b), which corresponds to a mixed phase with irregular atom arrangement. Lattice fringes of ca. 0.23 nm and ca. 0.26 nm are observed on the core and shell region, respectively; the former value corresponds to the (111) plane of pure Pd<sup>14</sup> while the other one corresponds to Zn metal (002) facet or Zn rich ZnPd alloy of closely similar lattice parameters.<sup>15</sup> This implies that the Pd surface was heavily doped with Zn atoms through the formation of a Pd@Zn bimetallic phase at the interface with high Zn content. In contrast, no core-shell structure was seen for sample 1 of similar size distribution of nanoparticles (5 wt% Pd, 0.0 wt% CdSe) (Figure S3) owing to the lower Zn content in this sample, which is consistent with the result of XPS. The extended X-ray absorption fine structure (EXAFS) results at Pd K-edge (24350 eV) are shown in Fig. 1c and SI (Figure S4 and Table S1). The direct observation of a shorter scattering path with 2.57 Å distance comparing with a typical 2.70 Å Pd-Pd scattering path<sup>16</sup> is assigned to the first shell scattering pair of

Pd-Zn. Meanwhile, the number of neighbouring Zn (NZn) around each absorbing Pd atom rises at the expense of neighbouring Pd (NPd) with increasing CdSe content. Clearly, from these results, the supported Pd@Zn bimetallic particles show intimate contact of the two elements which may modify the electronic structure of Pd in a subtle manner.

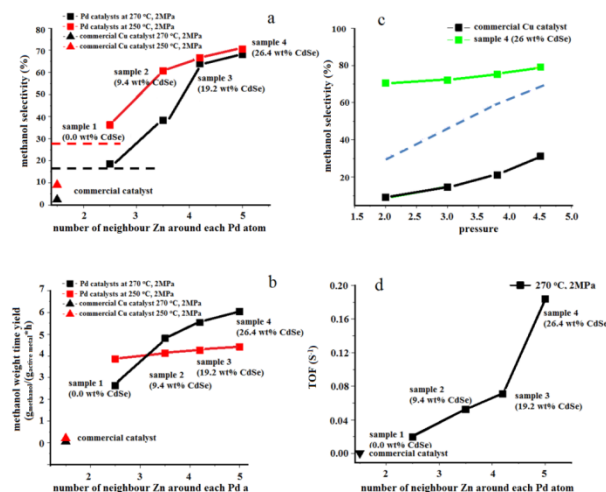


**Fig.2 a.** The plots of CH<sub>3</sub>OH selectivities; **b.** CH<sub>3</sub>OH weight time yields; for a series of Pd@Zn samples in CO<sub>2</sub> hydrogenation at 2.0 MPa with WHSV=18,000 mL h<sup>-1</sup>g<sup>-1</sup> versus number of NZn atoms around Pd derived from EXAFS at 250 °C (red) or 270 °C (black). Dotted line represents calculated thermodynamic selectivities (with taken both methanol synthesis and RWGS equilibria into account). **c.** The pressure effects on CH<sub>3</sub>OH selectivity for Pd@Zn (sample 4) and commercial Cu catalyst at 250 °C in range of 2- 4.5 MPa; **d.** TOF values of Pd in a series of Pd@Zn samples (5 wt% Pd) in CH<sub>3</sub>OH synthesis from CO<sub>2</sub> hydrogenation at 2.0 MPa, with WHSV=18,000 mL h<sup>-1</sup>g<sup>-1</sup>, with reference to commercial Cu catalyst.

The catalytic performances of the as-prepared Pd@Zn samples in CO<sub>2</sub> hydrogenation to methanol under a low pressure of 2MPa were studied (a mixture of CO<sub>2</sub>:H<sub>2</sub>=1:2.8 was flowed through the loaded catalyst (0.1g) in a fixed-bed reactor with a flow rate of 30 mL min<sup>-1</sup>). The plots of catalytic results of a series of Pd@Zn (5 wt% Pd) samples versus number of NZn atoms around Pd (derived from EXAFS) are summarized in Fig. 2. A commercial Cu/ZnO based catalyst (HiFUEL-R120 ~50wt Cu) was also employed as a reference. With the surface areas of Pd and Cu being taken into account (active sites per gram catalyst for Pd- and Cu-based catalysts are shown in Table S2), the methanol TOF were calculated (Fig. 2d); the values for Pd increase dramatically with respect to increasing Zn content (indicated by the number of NZn atoms around Pd from EXAFS), reaching 1.9×10<sup>-1</sup> s<sup>-1</sup> at sample 4, which is about 350 folds of that over the commercial Cu under same conditions.<sup>17</sup> As far as we are aware, this TOF values of sample 4 represent the highest TOFs among all the reported values using H<sub>2</sub>:CO<sub>2</sub> ratio of 3:1. The activity of sample 4 in term of weight-time yield has reached 6 g-methanol/g-active metal/h at 270 °C, 2.0 MPa (Fig. 2b) which is even much higher than the best reported value for Cu-based catalyst (1.48 g-methanol/g-active metal/h) over Cu/ZnO/Ga<sub>2</sub>O<sub>3</sub> (50 wt% Cu) at 5 MPa.<sup>12</sup> Comparing to our Cu catalyst of 0.1 g-methanol/g-active metal/h, it is 60 times higher than this commercial catalyst

under the same conditions.

Besides the activity (TOF), the methanol selectivity also dramatically increases according to the number of neighbour Zn in Pd@Zn catalysts (Fig. 2a). The nearly 80% methanol selectivity of sample 4 at 250 °C, 4.5 MPa is far beyond those of commercial Cu catalyst (30%) (Fig. 2c). It is even surprising to see sample 4 with the highest content of Zn(0) ( $N_{\text{Zn}}=5.0$ ) maintains a high methanol selectivity of 70% at 2 MPa with WHSV (weight hourly space velocity) = 18,000 mL h<sup>-1</sup>g<sup>-1</sup> (Fig. 2a,c). This clearly suggests the significance of the heavy decoration of Pd with Zn atoms, as Pd@Zn surface shows a sharp difference from the commercial Cu catalyst in the methanol synthesis; by decreasing the operational pressure from 4.5 MPa to 2.0 MPa (Fig. 2c), it is noted that methanol selectivity for the commercial Cu catalyst decreases sharply to under 10% which is governed by the thermodynamics. In contrast, methanol selectivities over such Pd@Zn catalyst especially at low pressures are well beyond the thermodynamic predicted data (indicated by the dotted line in Fig. 2c), indicating that the reaction rate of RWGS is significantly suppressed on the Zn rich Pd@Zn surface and is much lower than that of methanol synthesis. The apparent activation energies for RWGS on sample 4, conventional Pd/ZnO (sample 1) and the commercial Cu catalyst were indeed found to be 98 kJ/mol, 71 kJ/mol, 69 kJ/mol, respectively (the derivation of activation energy was based on catalytic data collected under 2 MPa at different reaction temperatures, see Figure S5-1 and Figure S5-2). The higher activation barrier of this Zn rich Pd@Zn catalyst promoted by CdSe (sample 4) for RWGS significantly decreases the CO production rate and promotes methanol selectivity comparing with conventional Pd/ZnO and Cu/ZnO. These results clearly indicate that Pd@Zn with high contents of Zn are promising low-pressure catalysts for methanol synthesis from CO<sub>2</sub> hydrogenation.

Fourier transform infrared (FTIR) spectroscopy shows some key surface intermediates and confirms the drastic attenuation in CO production on the Pd@Zn surface (Fig. 3). For sample 1 (shown in Fig. 3a, c), a series of vibration bands were detected including 2000 cm<sup>-1</sup>, 1860 cm<sup>-1</sup>, 1595 cm<sup>-1</sup>, 1395 cm<sup>-1</sup>, 1230 cm<sup>-1</sup>, 1502 cm<sup>-1</sup>, 1702 cm<sup>-1</sup> corresponding to adsorbed CO (linear mode, 2000 cm<sup>-1</sup> and bridge mode, 1860 cm<sup>-1</sup>)<sup>18</sup>, formate (1595 cm<sup>-1</sup>, 1395 cm<sup>-1</sup>)<sup>17</sup>, dioxymethylene (1230 cm<sup>-1</sup>)<sup>19</sup>, formaldehyde (1502 cm<sup>-1</sup>, 1702 cm<sup>-1</sup>)<sup>20</sup> species as similar to those previously reported over Cu surface. The signals of formate are observed at 50 °C and with rising temperature the vibration bands for CO, dioxymethylene and formaldehyde become more intense. For sample 4 (shown in Fig. 3b), almost no CO signal is detected even at 250 °C but the vibrations for dioxymethylene and formaldehyde clearly increase with increasing temperature. It is generally believed that the first step of CO<sub>2</sub>/H<sub>2</sub> activation generates two different surface intermediates of adsorbed HCOO and COOH, (note that the IR vibration bands of adsorbed COOH cannot be differentiated from that of HCOO due to the similar molecular structure) which leads to different reaction routes, as shown in Figure S6.<sup>21</sup> Hydrogenation of HCOO produces gaseous methanol via dioxymethylene and formaldehyde as intermediates, whereas decomposition of COOH yields gaseous CO product. The increasing signals of adsorbed CO with those of dioxymethylene and formaldehyde at elevated temperature imply the parallel progresses for CO and methanol synthesis on sample 1. The absence of CO signal confirms the suppressing of RWGS on sample 4 which may also reflect the selective blockage of CO<sub>2</sub> hydrogenation to COOH given that CO is formed from the decomposition of surface COOH.<sup>34</sup>

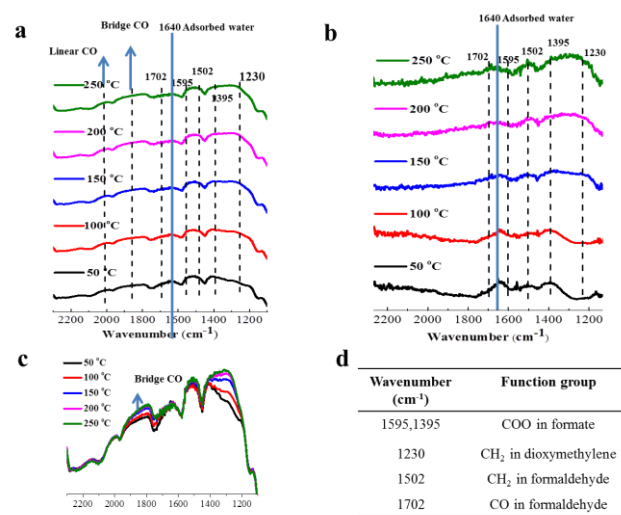


**Fig. 3** FTIR spectra of adsorbed species on reduced surface; **3a**, sample 1 (5 wt% Pd, 0.0 wt% CdSe); **3b** sample 4 (5 wt% Pd, 26.4 wt% CdSe) in CO<sub>2</sub> hydrogenation (A flow gas of 3 mol% CO<sub>2</sub> in H<sub>2</sub> was passed through the selected catalyst pellet of 20 mg) at variable temperatures; **3c**, The overlap of FTIR spectra for sample 1; **3d**, The assignments of vibration bands in FTIR. Both sample 1 and sample 4 were pre-reduced in H<sub>2</sub> at 250 °C for 1 h.

From the selected potential energy surfaces obtained from our density functional theory (DFT) calculations (the detailed calculation method is described in SI) as shown in Fig. 4, the occurrence of surface COOH is preferred over HCOO at pure Pd (111) (case A, Scheme S1) while with 2 ML Pd<sub>1</sub>Zn<sub>1</sub> (case D, 1 ML Zn coverage, Scheme S1) deposition, HCOO formation is much more favoured. Therefore, on sample 4 with the highest Zn content, the selective formation of HCOO over COOH as the intermediate leads to enhanced methanol selectivity through further multi-steps hydrogenation. It is also noted that the formation barrier of COOH on PdZn surface (1.43 eV) is higher than that on Pd(111) (1.21 eV) which implies the higher kinetic barrier for RWGS reaction since COOH is precursor of CO. The 0.22 eV difference corresponds to a 22 kJ/mol variation in activation energy of RWGS which is well consistent with the experimental value of 29 kJ/mol (refer to Figure S5-2).

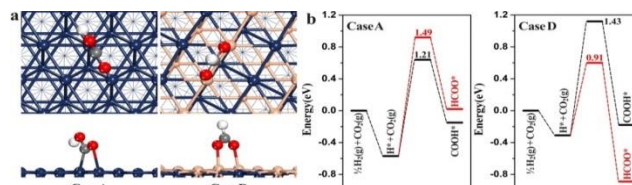


**Fig. 4 a**, The adsorption modes of COOH and HCOO on the Pd surfaces of cases A (pure Pd (111)), B (0.25 ML (monolayer) coverage of Zn), C (0.5 ML Zn), and D (1 ML of Zn), respectively were calculated. It is interesting to find that an entire monolayer of Zn at Pd (111) in case D is relatively less stable with respect to two mixed layers of Pd<sub>1</sub>Zn<sub>1</sub> (to form two mixed layers of Pd<sub>1</sub>Zn<sub>1</sub>/Pd(111)) indicative of more favourable formation of saturated surface alloy (in contrast to Cu system, see Figure S9). Thus, only case A and case D is compared (top: top view, bottom: side view); Pd and Zn atoms are in blue and orange, C, O and H atoms are in grey, red and white, respectively; **b**, Calculated energy profiles for CO<sub>2</sub> hydrogenation to adsorbed

COOH and HCOO at Pd cases A and D. (The numbers labelled in the figure are in unit of eV representing the corresponding reaction barriers.) The following profiles of COOH decomposition to CO are shown in Figure S7 which confirms the rapid CO formation from surface COOH species. Corresponding structures are shown in Figure S8.

It is interesting to observe a preferred formation of HCOO over that of COOH on Cu-based surfaces (noted the negative potential energy difference values of HCOO\* and COOH\* species shown in Table 1) as well as on PdZn surfaces but Cu-based surfaces exhibit much lower methanol selectivity than PdZn particularly under low pressure. Therefore, we calculated H adsorption at the various Pd and Cu surfaces. The results shown in Table 1 clearly showed that the H adsorption energies at Cu (111) decorated by Zn is quite low (0.16, 0.06 and -0.50 eV for case A, case D and case E, respectively; the structures of the Cu cases are shown in Figure S9), which render the Cu-based surfaces exhibiting lower activity in H<sub>2</sub> dissociation. At low operating pressure, this could lead to low coverage of surface H and slow down the further hydrogenation of HCOO into methanol. In addition, the decomposition of COOH to adsorbed CO and OH is less dependent on the concentration of surface H, which consumes the produced COOH in the first step rapidly and shifts the equilibrium between HCOO/COOH progressively. In contrast, Pd@Zn based surfaces show more superior ability in activating H<sub>2</sub> as indicated by the more favorable H adsorption energies (0.57 and 0.31 eV for case A and case D, respectively). Presumably this can further help to produce methanol readily from the hydrogenation of preferably formed HCOO under pressures as low as 2 MPa.

**Table 1.** Calculated H adsorption energies and energy differences of HCOO\* and COOH\* species on the Cu-based and Pd-based surfaces

Surface	case	H adsorption energy (eV)	E <sub>HCOO*</sub> -E <sub>COOH*</sub> (eV)
Cu-based	<b>A</b> (Cu (111))	0.16	-0.79
	<b>D</b> (2 ML Cu <sub>1</sub> Zn <sub>1</sub> / Cu (111))	0.06	-0.80
	<b>E</b> (1 ML Zn/ Cu (111))	-0.50	-1.11
Pd-based	<b>A</b> (Pd (111))	0.57	+0.18
	<b>D</b> (2 ML Pd <sub>1</sub> Zn <sub>1</sub> / Pd (111))	0.31	-0.70

## Conclusion

In conclusion, we have found that Zn enriched Pd@Zn core-shell bimetallic catalysts prepared via CdSe can stabilize surface HCOO species over COOH hence suppressing CO production from RWGS reaction during CH<sub>3</sub>OH formation from CO<sub>2</sub>/H<sub>2</sub>. The higher ability of this novel surface for H<sub>2</sub> adsorption and activation than Cu surface renders it more superior for methanol production from CO<sub>2</sub>/H<sub>2</sub> with methanol selectivity of over 70% even at 2.0 MPa. With the increasing demand for greener methanol synthesis from renewable resources, the superior catalytic performance of this novel Pd-based surface under low pressure may allow a more efficient method to couple with the

upstream CO<sub>2</sub>/H<sub>2</sub> production processes, as depicted in Scheme 1. It is believed that a new low pressure integrated methanol synthesis process at or below 2MPa can be further developed based on the above findings.

## Notes and references

- <sup>a</sup>Wolfson Catalysis Centre, Department of Chemistry, University of Oxford, Oxford, OX1 3QR, UK  
<sup>b</sup>Key Laboratory for Advanced Materials, Centre for Computational Chemistry and Research Institute of Industrial Catalysis, East China University of Science and Technology, Shanghai, P.R. China  
<sup>c</sup>State Key Laboratory of Physical Chemistry of Solid Surfaces, National Engineering Laboratory for Green Chemical Production of Alcohols-Ethers-Esters, iChEM, College of Chemistry and Chemical Engineering, Xiamen University, Xiamen 361005, China.  
<sup>d</sup>Diamond Light Source Ltd, Harwell Science and Innovation, Chilton, Didcot, Oxfordshire, OX11 0DE, UK  
<sup>e</sup>Department of Chemistry, Wuhan University, Wuhan 430072, P.R. China

The authors wish to thank EPSRC, UK (Oxford) and NSFC-21421004, 21373153, 21322307, China and iChEM consortium, China for the financial support of this collaborative work and are grateful to Chinese Scholarship Council (CSC) of China to grant a PhD scholarship to FL to work at Oxford. The ECUST group also thank the computing time in National Super Computing Center in Jinan.

<sup>†</sup>Electronic Supplementary Information (ESI) available: details in sample preparation, testing and characterization, see DOI:

- G. A. Olah, *Angew. Chem. Int. Ed.* 2005, **44**, 2636–2639.
- L. K. Rihko-Struckmann, A. Peschel, R. Hanke-Rauschenbach & K. Sundmacher, *Ind. Eng. Chem. Res.* 2010, **49**, 11073–11078.
- J. Wu, M. Saito, M. Takeuchi, T. Watanabe, *Appl. Catal. A Gen.* 2001, **218**, 235–240.
- G. C. Chinen, P. J. Denny, J. R. Jennings, M. S. Spencer, & K. C. Waugh, *Appl. Catal.* 1988, **36**, 1–65.
- J. R. Rostrup-Nielsen, *Catal. Today* 1993, **18**, 305–324.
- G. A. Olah, 2009, *Science* **203**, 34–35.
- R. D. Cortright, R. R. Davda, J. A. Dumesic, *Nature*, 2002, **418**, 964–967.
- A. J. Esswein, & D. G. Nocera, Hydrogen production by molecular photocatalysis. *Chem. Rev.* 2007, **107**, 4022–4047.
- L. M. Romeo, *et al. Energy Convers. Manag.* 2008, **49**, 2809–2814.
- G. Bolye, Renewable Energy—Power for a Sustainable Future, Oxford University Press: Oxford, UK, **1996**.
- R. R. Davda, J. W. Shabaker, G. W. Huber, R. D. Cortright & J. A. Dumesic, *Appl. Catal. B Environ.* 2005, **56**, 171–186.
- M. Saito, *Catal. Surv. Jpn.* 2000, **2**, 175–184.
- Y. Yang, J. Evans, J. A. Rodriguez, M. G. White & P. Liu *Phys. Chem. Chem. Phys.* 2010, **12**, 9909–9917.
- J. Zhang, Y. Xu, B. Zhang, *Chem. Commun.* 2014, **50**, 13451–13453.
- D. Pradhan, S. Sindhwani, K. T. Leung, *J. Phys. Chem. C* 2009, **113**, 15788–15791.
- S. Takenaka, Y. Shigeta, E. Tanabe, K. Otsuka, *J. Catal.* 2003, **220**, 468–477.
- J. Araña *et al. Appl. Surf. Sci.* 2004, **239**, 60–71.
- A. Karelavic, *ACS Catal.* 2013, **3**, 2799–2812.
- T. Chen, *et al. J. Phys. Chem. C* 2007, **111**, 8005–8014.
- G. Y. Popova, T. V. Andrushkevich, Y. A. Chesalov, E. S. Stoyanov, *Kinet. Catal.* 2000, **41**, 885–891.
- Y.-F. Zhao *et al. J. Catal.* 2011, **281**, 199–211.